Some Properties of "Madrid" Liquids†

Dongxu Li and Stuart A. Rice*

Department of Chemistry and The James Franck Institute, The University of Chicago, Chicago, Illinois 60637

Received: May 19, 2004; In Final Form: September 17, 2004

It has recently been suggested that stratification of the liquid−vapor interface may be a general structural characteristic of liquids that have a very small ratio of melting temperature to critical temperature, and a pair additive potential that generates a small ratio of melting temperature to critical temperature and a stratified liquid−vapor interface has been developed. In this paper, we examine whether a density independent pair potential that supports a stratified liquid−vapor interface also supports liquid and solid phases with realistic structures and properties. We describe a class of potential energy functions that support "Madrid" liquids, and we report the results of simulations of both the liquid−vapor interface structures and the bulk structures of two such liquids. One of the interesting results obtained is that a "Madrid" potential generates a solid that supports a premelting stage in the melting transition. Since, of simple substances composed of either atomic or very compact molecular species, it is only the liquid−vapor interfaces of metals that are stratified, our analysis addresses whether a density independent potential energy function can simultaneously account for the structures and properties of the liquid−vapor interface and the bulk phases of a metal. We show that even though a Madrid liquid can have a stratified liquid−vapor interface, and thereby resemble a liquid metal, other properties of the Madrid liquid do not agree with the known properties of a liquid metal.

1. Introduction

It is a fundamental tenet of the molecular theory of matter that all of the properties of a system are fully determined by the form of the potential energy function. When classical mechanics is a valid description, it is also commonly assumed that the intramolecular potential energy and the intermolecular potential energy are separable (i.e., that the internal states of the molecules are not influenced by the spatial and orientation distributions of the molecules). Then, the structure and the thermodynamic properties of the liquid are determined by the intermolecular potential energy function. However, different properties of the liquid are sensitive to different extents to the detailed character of the potential energy function. The most widely used assumption is that the potential energy function can be represented as a sum of pair interaction functions. This approximation is rather good for a simple liquid, such as Ar, but even in such a case it is known that the potential energy function contains some contribution from three particle interactions.[1] Even when those multiparticle interactions are weak, it is frequently found that an effective pair potential, defined with parameters that are density dependent, will yield a good description of one property of the liquid, say the pair correlation function, although failing to provide an equally accurate prediction of some other property of the liquid, say the internal energy.[2] A caricature potential that provides a good example of this behavior is the hard sphere interaction. Although it is commonly found that a hard-core interaction with density dependent diameter can describe the pair correlation function of a dense simple liquid with rather good accuracy, that potential (obviously) gives a very inaccurate prediction of the internal energy of the liquid. The lesson to be drawn is simple: agreement between the measured value of a property of a liquid and that predicted with use of a particular intermolecular potential energy function does not unambiguously verify the accuracy of that particular intermolecular potential energy function.

These rather elementary observations are relevant to recent discussions concerning the relationship between the layering at a free liquid surface and the character of the intermolecular potential energy function that supports said layering.[3] The liquid−vapor interface is a naturally supported inhomogeneous fluid. The seminal work of van der Waals,[4,5] based on a representation of the chemical potential of the inhomogeneous fluid that includes dependence on the gradient of the density, predicts that this interface has a density distribution with monotone decay from the bulk liquid density to the vapor density over a distance that depends on the system temperature. When the system temperature is close to the freezing temperature, that distance is a few molecular diameters. The van der Waals theory is macroscopic in character, and there has been concern about the validity of the representation of the chemical potential when the density gradient in the interface is large, as is the case for the liquid−vapor interface near the freezing temperature. However, for the case of dielectric liquids, more recent microscopic theories of the structure of the inhomogeneous liquid−vapor interface, based on integral equation representations of the density distribution[6] and on simulation studies,[7] confirm all of the essential features of the van der Waals analysis.[4,5] Experimental studies of the density distribution along the normal to the liquid−vapor interface of a dielectric liquid also confirm the predictions of the van der Waals analysis.[8]

When the liquid is a metal, the density profile along the normal to the free surface is different. It was first predicted,[9−11] then confirmed experimentally,[12−17] that the density distribution along the normal to the liquid−vapor interface of a metal is

* Author to whom correspondence should be addressed. E-mail: sarice@uchicago.edu.

† Part of the special issue "Frank H. Stillinger Festschrift".

10.1021/jp040367g CCC: $27.50
Published on Web 11/16/2004

layered to a depth of three to four atomic diameters. The characteristic feature of the potential energy function that supports this structure is its dependence on electron density. In the pseudopotential representation of the energy of the metal, it is the dependence of the one-body term in the potential energy on the electron density that dominates the overall density dependence of the system energy and that is responsible for the observed stratification of the liquid−vapor interface.[9−11] This strong density dependence of the potential energy function differentiates a metal from a dielectric because the effective intermolecular interaction in the latter case is only very weakly density dependent.

This paper examines whether an ad hoc density independent pair potential that supports stratification of the liquid−vapor interfaces is appropriate for liquid metals. The investigation consists of determining whether other properties of the liquid supported by such a potential are consistent with known properties of liquid metals. The context of this issue is as follows. Recently, Velasco, Tarazona, Reinaldo-Falagán, and Chacón[3] have suggested that stratification of the liquid−vapor interface may be a general structural characteristic of liquids that have a very small ratio of melting temperature to critical temperature. Put another way, the suggestion is that the electron density dependence of the potential energy of a metal generates, typically, a very small ratio of melting temperature to critical temperature and that it is the latter macroscopic feature of the equilibrium field of the liquid state that determines the existence or nonexistence of stratification of the liquid−vapor interface. They have invented a potential energy function that generates a small ratio of melting temperature to critical temperature and a stratified liquid−vapor interface. We hereafter call liquids that have this form of pair interaction "Madrid" liquids. The question we address is whether other properties of the liquid state supported by a Madrid potential energy function are similar to or differ from those of a conventional liquid.

We take the view that the Madrid potential energy function defines a new class of liquids with properties somewhat different from conventional liquids. In this paper, we examine whether a density independent pair potential that supports a stratified liquid−vapor interface also supports liquid and solid phases with realistic structures and properties. We describe a class of potential energy functions that support Madrid liquids, and we report the results of simulations of both the liquid−vapor interface structures and the bulk structures of two such liquids. One of the interesting results obtained is that a Madrid potential generates a solid that supports a premelting stage in the melting transition. Since, of simple substances composed of either atomic or very compact molecular species, it is only the liquid−vapor interfaces of metals that are stratified, our analysis addresses whether a density independent potential energy function can simultaneously account for the structures and properties of the liquid−vapor interface and the bulk phases of a metal. We show that even though a Madrid liquid can have a stratified liquid−vapor interface, and thereby resemble a liquid metal, other properties of the Madrid liquid do not agree with the known properties of a liquid metal.

2. Class of Flat Bottom Potentials

The observed melting point to critical point ratio, T_m/T_c, is about 0.5 for a dielectric fluid and about 0.15 for a low melting point metal.[18] Velasco and co-workers[3] have constructed a class of model pair potentials that supports liquids with a small value of T_m/T_c. Their pair potential for Na is

$$\phi(r) = A_0\, e^{-\alpha r} - A_1\, e^{-\beta(r-R_1)2} \quad (1)$$

with $A_0 = 5.077 \times 10^6$ K, $A_1 = 2131$ K, $\alpha = 22.322$ nm^{-1}, $\beta = 21.4$ nm^{-2}, and $R_1 = 0.35344$ nm. As shown in Figure 1, this potential is rather flat in the vicinity of its minimum relative to, say, a Lennard-Jones potential. In addition, the potential is rather short ranged, because the exponential form of the attractive component tends to zero much more rapidly than does the r^{-6} interaction of the Lennard-Jones potential.

We now focus attention on a class of potentials that satisfy the conditions

$$\frac{du_2(r)}{dr} = 0, \quad \frac{d^2u_2(r)}{dr^2} = 0, \quad \frac{d^3u_2(r)}{dr^3} = 0 \quad (2)$$

at the minimum of $u_2(r)$. Two examples of such potentials are also displayed in Figure 1. Their functional forms are, as functions of the reduced distance $x = r/\sigma$,

$$u_2(r)/\epsilon = \frac{e^4}{(2\pi^4 - \pi^2)e^{6x}\, x}\{[2\, e^2\, \pi^2(5 + 2\pi^2) - 3\, e^{2x}(-2 + 7\pi^2 + 2\pi^4)]x + 6\, e^{2x}(-1 + 2\pi^2)x \cos(2\pi x) + 12\, e^{2x}\, \pi \sin(2\pi x)\} \quad (3)$$

$$u_2(r)/\epsilon = 10\, e^4\left(\frac{2}{5}e^{6-10x} - \frac{3}{2}e^{4-8x} + 2e^{2-6x} - e^{-4x}\right) \quad (4)$$

The potential depth, ϵ, and the length scale of the interaction, σ, were chosen so that these pair potentials are similar to the Madrid pair potential. This is achieved by setting $\epsilon = 0.18382$ eV $= 2133$ K and $\sigma = 0.4862$ and 0.4565 nm, respectively, for the model potentials I and II.

3. Computational Details

We have carried out Monte Carlo simulations of the behavior of systems with the two pair potentials described in the last section. Our simulation samples contained 14 000 molecules, initially arranged in 20 layers in a box whose length in the z direction was chosen to be several times larger than the thickness of the liquid sample. The simulation box side lengths in the x and the y directions were determined by the density of molecules in the interior layers of the sample. Periodic boundary conditions were applied to all three directions of the simulation box. Note that the box length in the z direction is great enough that the use of a periodic boundary condition does not affect the liquid−vapor interface (i.e., the boundaries in the z-direction are deep in the vapor phase).

All of the simulations were started from random configurations of molecules without overlaps. Usually, it took at least one million Monte Carlo passes to equilibrate the system. In our terminology, one Monte Carlo pass involves the displacement of each of the 14 000 molecules in the simulation sample. For each phase, the bulk densities were calculated at the center of each phase and for a z range of about 10% of the box length in the z direction.

We have calculated the coexistence line in the temperature−density plane, the bulk pair correlation functions of the liquids, the pair correlation functions as a function of position in layers parallel to the liquid−vapor interface, and the predicted X-ray reflectivity of the liquid−vapor interface. We use these data to characterize the Madrid liquids and to demonstrate some of the

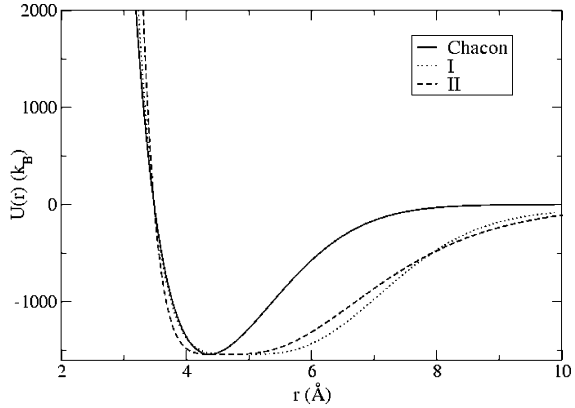

Figure 1. The two flat bottom model potentials used in our simulations. For comparison, the model potential constructed for Na by Velasco et al.[3] is also shown.

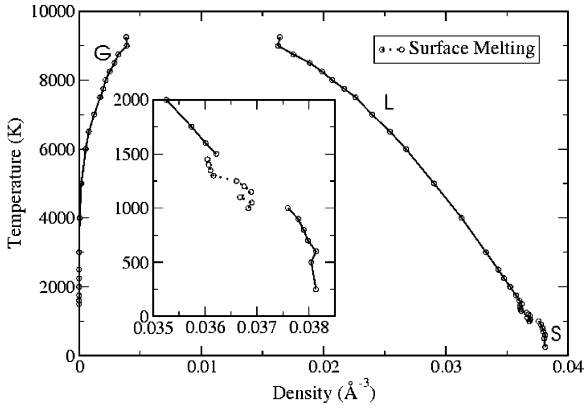

Figure 2. The phase diagram calculated for model system I. The dotted line indicates surface melting. The inset shows the behavior around the melting point. The lines shown are intended to be a the guide for the eye.

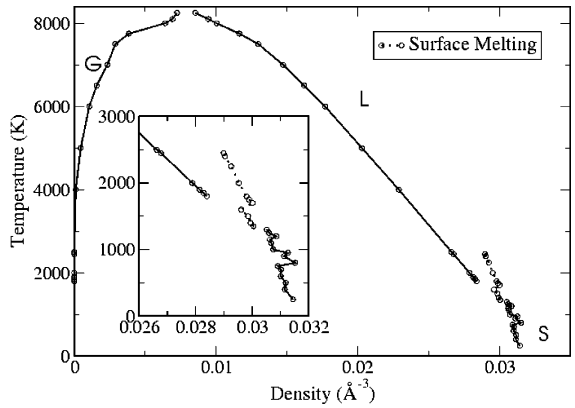

Figure 3. The phase diagram calculated for model system II. The dotted line indicates surface melting. The inset shows the behavior around the melting point. The lines shown are intended to be a guide for the eye.

differences between their properties and the properties of conventional liquids.

4. Results

Figure 1 displays the two model pair potentials (I and II) that determine the properties of the systems that we have simulated, and Figures 2 and 3 display the phase diagrams for those systems. The melting temperatures of systems I and II are estimated to be 1450 and 2450 K, respectively. System I exhibits a small increase in bulk density on melting, namely,

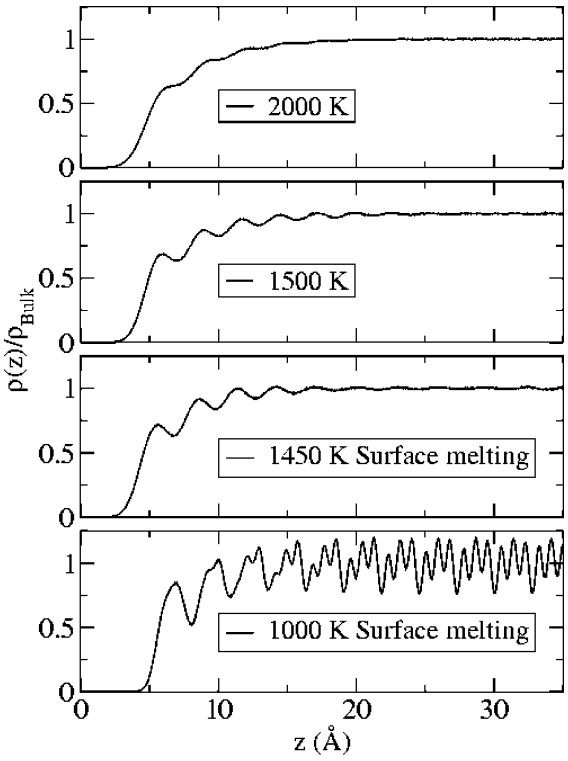

Figure 4. The longitudinal density profiles for the model system I. The system is in a surface melting state at temperatures 1000 and 1450 K.

0.5%, whereas system II exhibits a 7% decrease in bulk density on melting. The ratios of melting point to critical point are found to be 0.16 and 0.32, respectively, for the systems supported by model potentials I and II. The critical temperatures of these liquids were obtained by extrapolation of the liquid−vapor coexistence curve and are estimated to be 9550 and 8135 K for systems I and II, respectively.

The longitudinal density distributions in the liquid−vapor interfaces of Madrid liquids I and II, displayed in Figures 4 and 5, clearly show stratification, the more so the lower the temperature. Note that the densities of the layers are lower than the bulk density. In system I, the densities of the two outermost strata are 0.59 and 0.79 of the bulk density at 1500 K; in system II, the densities of the two outermost strata are 0.63 and 0.85 of the bulk density at 1800 K. These relative densities are somewhat smaller than that found for the liquid−vapor interface supported by the original Madrid potential. More important, the shapes of the envelopes of the maximum densities of the strata in the liquid−vapor interfaces of Madrid liquids I and II are different from that found for the liquid−vapor interface of a metal. In the latter case, the strata in the liquid−vapor interface have peak densities that are larger than the bulk density and that usually decrease in magnitude from the outermost stratum into the bulk liquid.

An unexpected result of our simulations is the finding that the systems supported by model pair potentials I and II undergo surface melting in a well-defined region of the temperature−density plane; that region is shown by dotted lines in Figures 2 and 3. This inference is drawn from an examination of the pair correlation functions in the several strata of the longitudinal density profiles shown in Figures 4 and 5; these pair correlation functions are shown in Figures 6 and 7 for thermodynamic states of systems I and II in the liquid region and in Figures 8 and 9 for thermodynamic states of systems I and II in the surface melting region.

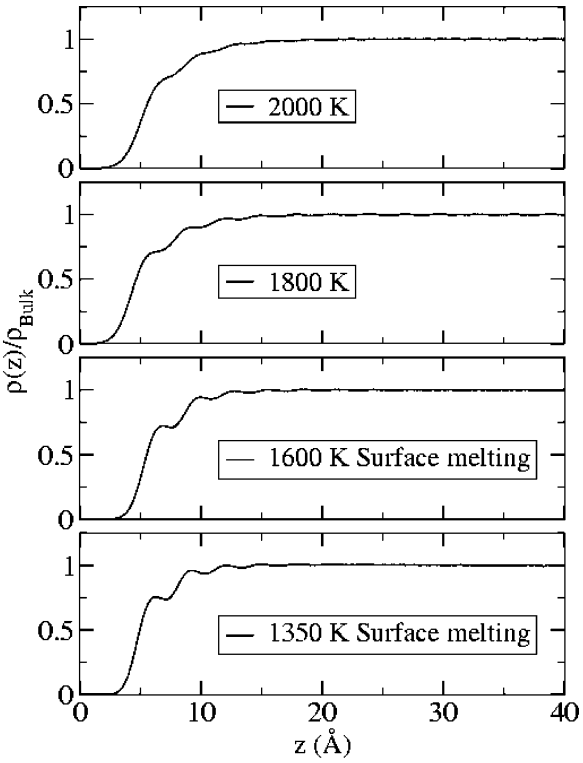

Figure 5. The longitudinal density profiles for the model system II. The system is in a surface melting state at temperatures 1350 and 1600 K.

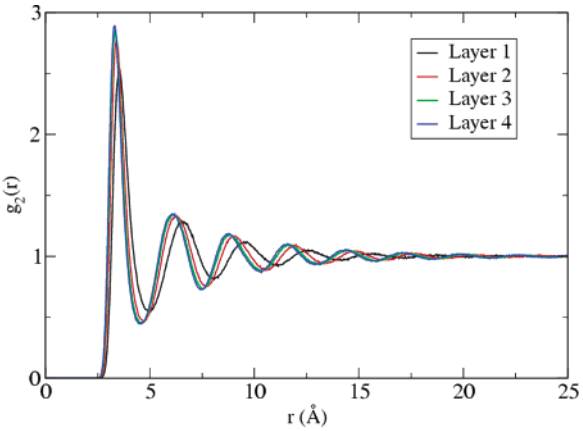

Figure 6. The pair correlation functions in the outermost layers for at the liquid−vapor interface at 1500 K, for the model system I.

In the liquid region (Figures 6 and 7), these pair correlation functions show that the nearest neighbor spacing increases as one goes from the innermost to the outermost layer of the stratified liquid−vapor interface. In the surface melting region (Figures 8 and 9), the pair correlation functions for the outermost layers in both systems I and II are characteristic of a liquid, whereas they are characteristic of a solid by layer 2 of system I and by layer 3 of system II. Figures 10 and 11 display snapshots with which one can compare the coordination of the atoms in the outermost layer of each system with that of a layer in the bulk of that system for a thermodynamic state in which surface melting occurs. The representation shown is of the Voronoi polygon segmentation of the layer of atoms. In this representation, the number of sides of the polygon that encloses a point (atom) gives the in-plane coordination number. It is clearly seen that the bulk phases of system I at 1450 K and of system II at 1300 K are crystalline, but that the outermost layer of each system has many deviations from perfect hexagonal

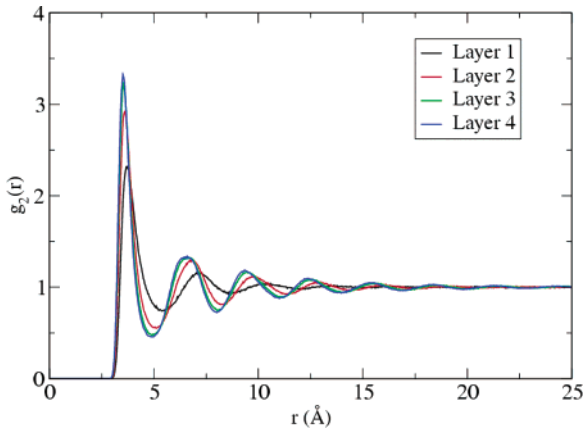

Figure 7. The pair correlation functions in the outermost layers for the liquid−vapor interface for the model system II. The bulk is supercooled at 1800 K.

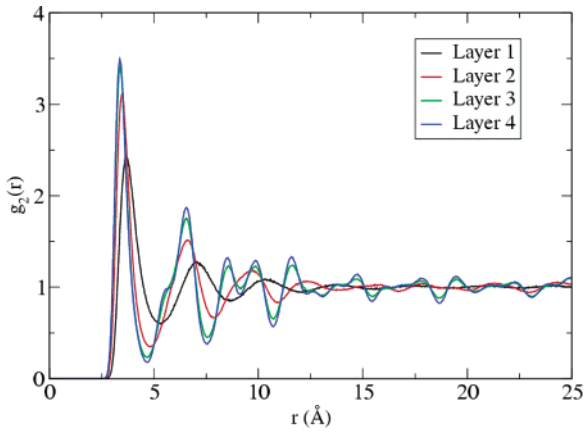

Figure 8. The pair correlation functions at 1450 K in the outermost layers of the liquid−vapor interface of model system I. This figure is an analogue of Figure 6 for a state that exhibits surface melting.

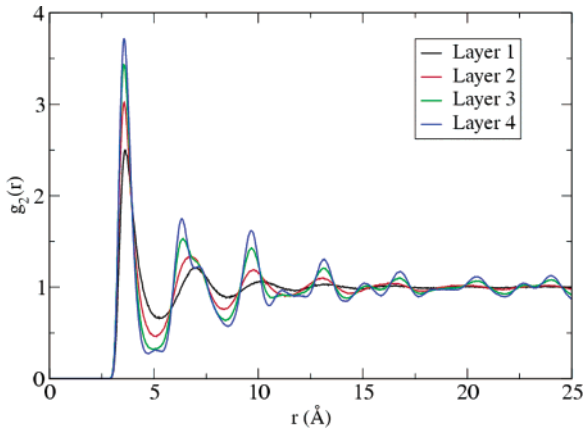

Figure 9. The pair correlation functions at 2250 K in the outermost layers of the liquid−vapor interface of model system II. This figure is an analogue of Figure 7 for a state that exhibits surface melting.

packing, as is typical of a premelted layer. We note that, because of the limited size of the simulation box, the surface phase transition is associated with density changes in the bulk solid. For system I, the bulk density decreases by about 3% when surface melting occurs. For system II, the bulk density increases by about 0.2% when surface melting occurs.

We have already remarked that the shapes of the longitudinal density distributions in the liquid−vapor interfaces of these Madrid liquids are different from those inferred for the liquid−vapor interfaces of metals. This difference has experimental

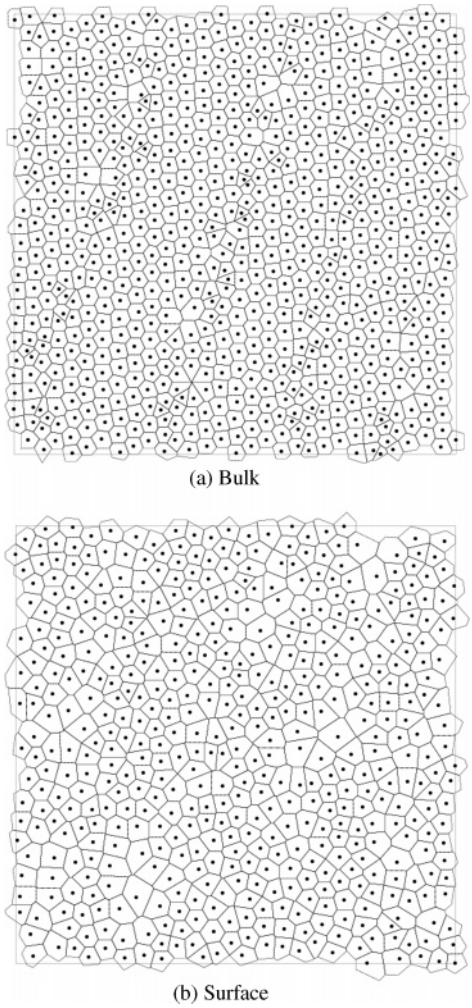

Figure 10. Instantaneous configurations of the outermost layer and a bulk layer of system I at 1450 K. The configuration has been segmented with Voronoi polygons to show the order within the layer.

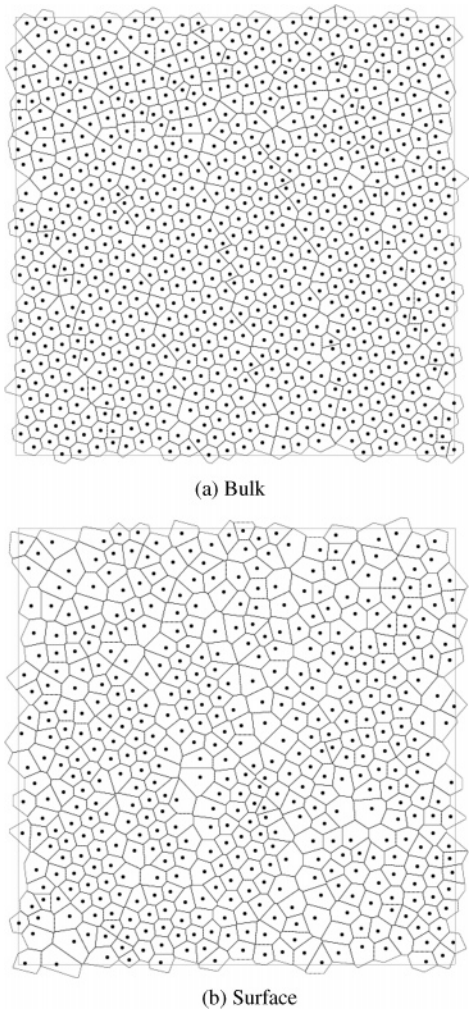

Figure 11. Instantaneous configurations of the outermost layer and a bulk layer of system II at 1300 K. The configuration has been segmented with Voronoi polygons to show the order within the layer.

consequences. To illustrate one such consequence, we have calculated the X-ray reflectivity as a function of out-of-plane momentum transfer with magnitude of wave vector, q_z, for the liquid−vapor interfaces of systems I and II, and compared those results with the X-ray reflectivity calculated for a model liquid−vapor interface of a metal. The model of the liquid metal−vapor interface we use has strata with constant density, equal to the bulk value, and increasing in width as one goes away from the outermost stratum into the bulk liquid. This model has peak densities in excess of the bulk density when the width of the layer is small, and these peak densities decay to the bulk density when the width of the layer becomes large; the decay occurs in about four layers. We have used the distorted crystal representation of this model because it has a simple analytic form and it can be parametrized to fit the experimental data for the longitudinal density distribution in the liquid−vapor interface of a metal very well.[12,13,19] The results are shown in Figures 12 and 13. Although the X-ray reflectivity of the liquid−vapor interfaces of the Madrid liquids and of the distorted crystal representation of a typical liquid metal agree at large q_z, there are very large differences over most of the experimentally accessible range of q_z. Note that the high-frequency ripples in the reflectivity of the liquid−vapor interfaces of systems I and II that appear in these figures are an artifact arising from the limited size of the simulation box.

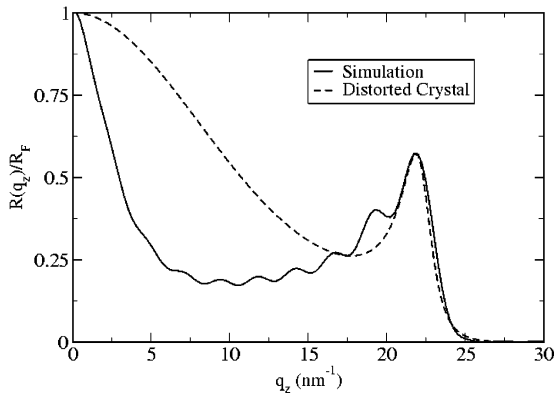

Figure 12. The calculated X-ray reflectivity of the liquid−vapor interface of system I (solid line) compared with the calculated X-ray reflectivity of the liquid−vapor interface represented by the distorted crystal model (dashed line). The temperature is 1500 K, which is just above the melting point of system I.

The behavior of the crystal phases of systems I and II is complex. The bulk pair correlation functions of crystalline phases of systems I and II are plotted together with the locations of the atoms in ideal body-centered-cubic (bcc) and face-centered-cubic (fcc) lattices in Figures 14 and 15, respectively. The low-temperature lattice structure of system I is bcc. When surface melting occurs at 1000 K, it is accompanied by a structural transition of the bulk from bcc to fcc. The fcc structure with a premelted surface layer is stable up to 1250 K. Between 1300 and 1450 K, the pair correlation functions within layers

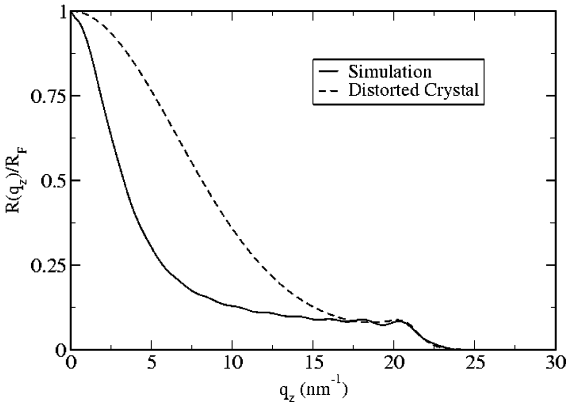

Figure 13. The calculated X-ray reflectivity of the liquid−vapor interface of system II (solid line) compared with the calculated X-ray reflectivity of the liquid−vapor interface represented by the distorted crystal model (dashed line). The temperature is 1800 K, which is in the supercooled region.

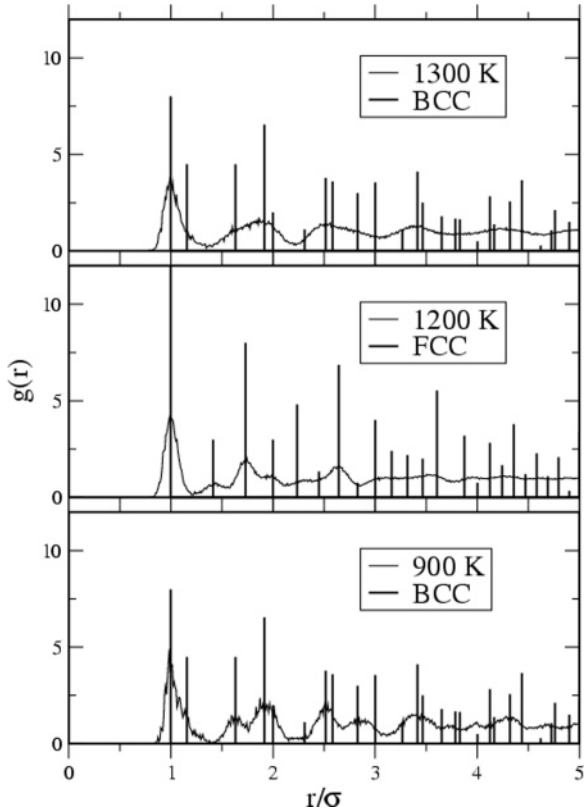

Figure 14. Pair correlation functions for the bulk phase of system I at several temperatures. The vertical lines show the positions of atoms in perfect face-centered-cubic (fcc) and body-centered-cubic (bcc) lattices. The pair correlation functions have been normalized to ease the comparison.

parallel to the interface show that the two outermost layers are in a liquidlike state, whereas for deeper layers the pair correlation functions indicate that the bulk structure is close to bcc.

5. Final Comments

The Madrid potential belongs to a class of potentials that have very flat minima. Pair potentials with this unusual shape support liquid and solid properties that are different from those commonly found. Thus, we have found that although these potentials predict that the liquid−vapor interface is stratified that stratification exhibits qualitative differences with the stratified liquid−vapor interfaces of metals. We expect that another consequence

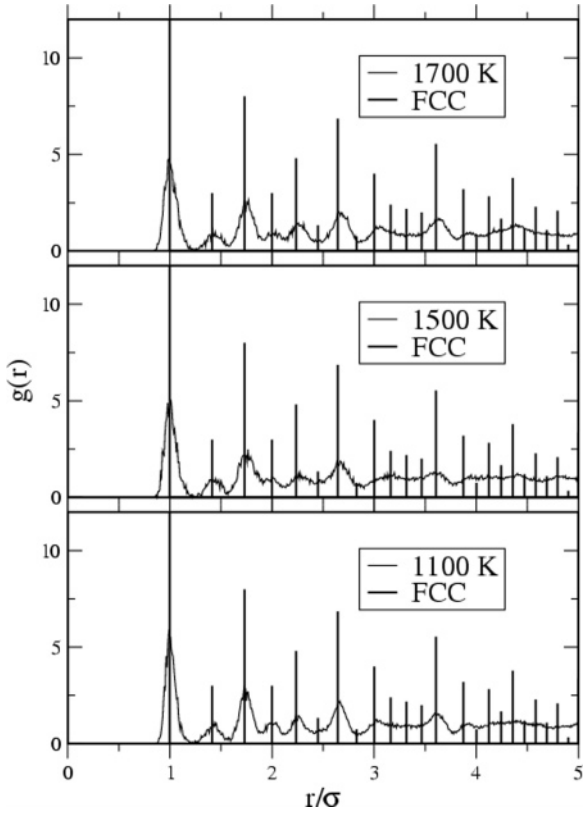

Figure 15. Pair correlation functions for the bulk phase of system II at several temperatures. The vertical lines show the positions of atoms in a perfect face-centered cubic lattice. The pair correlation functions have been normalized to ease the comparison.

of the very flat minimum in a Madrid pair potential will be a phonon spectrum of the solid that is rather different from the typical phonon spectrum. In general, we argue that "Madrid" potentials support a class of liquids and solids that have properties that are very different from those of liquids and solids supported by conventional pair potentials, such as the Lennard-Jones potential. One example of such a difference is the existence of premelting in the solid-to-liquid transition. We suspect that there are many other such differences and that further study of systems supported by Madrid potentials can reveal interesting and unsuspected properties of matter.

Acknowledgment. This research was supported by a grant from the National Science Foundation.

References and Notes

(1) Bukowski, R.; Szalewicz, K. *J. Chem. Phys.* **2001**, *114*, 9518.

(2) Martynov, G. A. *Fundamental Theory of Liquids: Method of Distribution Functions*; A. Hilger: Bristol, 1992.

(3) Velasco, E.; Tarazona, P.; Reinaldo-Falagán, M.; Chacón, E. *J. Chem. Phys.* **2002**, *117*, 10777.

(4) Rowlinson, J. S. *J. Stat. Phys.* **1979**, *20*, 197.

(5) Rowlinson, J. S.; Widom, B. *Molecular Theory of Capillarity*; Clarendon: Oxford, 1982.

(6) Evans, R.; In *Fundamentals of Inhomogenous Fluids*; Henderson, D., Ed.; M. Dekker: New York, 1992; Chapter 3, pp 85−175.

(7) Henderson, D. In *Fundamentals of Inhomogenous Fluids*; Henderson, D., Ed.; M. Dekker: New York, 1992; Chapter 4, pp 177−199.

(8) Braslau, A.; Deutsch, M.; Pershan, P. S.; Weiss, A. H. *Phys. Rev. Lett.* **1985**, *54*, 114.

(9) D'Evelyn, M. P.; Rice, S. A. *J. Chem. Phys.* **1983**, *78*, 5225.

(10) D'Evelyn, M. P.; Rice, S. A. *J. Chem. Phys.* **1983**, *78*, 5081.

(11) D'Evelyn, M. P.; Rice, S. A. *Phys. Rev. Lett.* **1981**, *47*, 1844.
(12) Regan, M. J.; Kawamoto, E. H.; Lee, S.; Pershan, P. S.; Maskil, N.; Deutsch, M.; Magnussen, O. M.; Ocko, B. M.; Berman, L. E. *Phys. Rev. Lett.* **1995**, *75*, 2498.
(13) Tostmann, H.; DiMasi, E.; Pershan, P. S.; Ocko, B. M.; Shpyrko, O. G.; Deutsch, M. *Phys. Rev. B* **1999**, *59*, 783.
(14) Shpyrko, O.; Huber, P.; Grigoriev, A.; Pershan, P.; Ocko, B.; Tostmann, H.; Deutsch, M. *Phys. Rev. B* **2003**, *67*, 115405.
(15) Regan, M. J.; Pershan, P. S.; Magnussen, O. M.; Ocko, B. M.; Deutsch, M.; Berman, L. E. *Phys. Rev. B* **1997**, *55*, 15874.
(16) Lei, N.; Huang, Z.; Rice, S. A. *J. Chem. Phys.* **1995**, *104*, 9606.
(17) Lei, N.; Huang, Z.; Rice, S. A. *J. Chem. Phys.* **1997**, *107*, 9606.
(18) Lide, D. R., Ed. *CRC Handbook of Chemistry and Physics*; CRC Press: Boca Raton, FL, 2004.
(19) Zhao, M.; Checkmarev, D. S.; Cai, Z.-H.; Rice, S. A. *Phys. Rev. E* **1997**, *56*, 7033.